Proceedings of the Sixth IASTED International Conference
EUROPEAN POWER AND ENERGY SYSTEMS
June 26–28, 2006, Rhodes, Greece

A SIMULATOR FOR SINGLE PHASE INDUCTION MOTOR-CONVERTER PERFORMANCE

*L. Ben Amor, Electrical Engineering Department
**C. A. Belhadj, Electrical Engineering Department
**S. El Ferik, Systems Engineering Department
**A. S. Hussain, Systems Engineering Department

**King Fahd University of Petroleum and Minerals
Dhahran 31261, Saudi Arabia

* College of Technology at Dammam
Dammam, Saudi Arabia

ABSTRACT
This paper presents a simulator suitable for both transient and steady state performance prediction of a single phase induction motor (SPIM). The powerful Sim-Power - Systems Blockset is used as a simulation platform. The SPIM model includes representation of both main and auxiliary winding in stationary reference frame. The simulator includes a Triac based ac power converter. Both currents and voltage waveforms can be simulated for different firing angles. The simulator allows both current-speed and torque-speed characteristics calculation. Direct and soft starting tests were performed on a SPIM driven window type air conditioning unit. The simulated and experimental tests are compared showing close agreement.

KEY WORDS
SPIM simulator, steady state characteristics, transient operation analysis, air conditioning unit, soft starting.

1. Introduction

Single-phase induction motors (SPIM) are the most rugged and most widely used motors in the world. They are mostly used in residential appliances such as air-conditioners, refrigerators, pumps and so fourth. With the new technology being introduced such as adjustable speed drives, modeling, simulation and control of small induction machines such as the SPIM is of growing concern to engineers.

Although simpler in construction, SPIM is inherently more complex to model and to analyze. In the literature there is no abundance of results that have been published on motor modeling simulation and control.

A computer simulation of the SPIM operating in the motoring, generating and braking modes was presented in [1]. Tow dimensional finite element theory in conjunction with time stepping and rotor mesh movement was used. The developed software was tested on a capacitor-start SPIM. The model has been shown to reproduce the effects of continuous rotation of the real machine at both constant and variable speed.

The dynamical operation of the SPIM was curried out by applying a general method for coupling field and electrical circuit equations [2]. Two dimensional finite element methods were used to solve the electromagnetic field equations while electrical circuit equation representing the feeding circuit was written in a matrix form. The limitation of such simulation method is that all the equations associated to the feeding circuit had to be derived manually. This could be a difficult task when complex power converter and control strategies are used in the motor drive.

In [3], the machine equations were solved using a digital algorithm according to Electromagnetic Transients Program (EMTP). All mechanical components were converted to electrical components, put into one matrix, and solved by gauss elimination method. The effect of starting and/or run-capacitor on motor torque pulsation has been investigated. However, the Universal Machine (UM) model used to simulate capacitor SPIM did not take into account harmonics resulting from slot effect. Moreover, the model considers switches as ideal devices.

In [4], dynamic operation of the SPIM was studied using PSPICE software. The machine dynamics were presented by a set of nonlinear time-varying differential equations. The equations, which define the motor operation, were represented in an orthogonal system. The electric circuit presenting this set of equations is determined and solved by PSPICE software. The simulation results were compared with those obtained by EMTP as well as those obtained by experiments. Good agreements were observed for both cases.

The Phasor-Dynamic Approach (generalized averaging) technique was applied for dynamical and steady-state modeling of single-phase induction machine [5]. Each state variable was expressed in terms of Fourier series with slowly time varying coefficients. The drawback of such technique is that it allows only identifying phenomena associated with the fundamental frequency under constant load torque.

In [6], a Triac bridge circuit was used to implement electronic pole-changing speed control. Usual stator reference frame dq-axis dynamic simulation model was applied [7]. An ideal transformer has been added to account for different effective numbers of turns in the main and auxiliary windings. The simulator was however built using motor and the power converter dynamic equations witch were developed manually then integrated using the Advanced Continuous Simulation Language (ACSL). Moreover, integration procedure must handle transitions between different circuit operation modes.

When the motor voltage, current, and frequency must be varied as required by most industrial applications, the SPIM should be coupled with a power converter. Different equations must then be developed for each switching state of the power converter. The number of equations representing the converter dynamics during one operating cycle depends on both converter configuration and switching control strategy. Manual derivation of these equations may not be an easy task. To overcome such heavy analytical development we propose to simulate the converter driven motor system using the powerful SimPowerSystems Blockset.

The paper is organized as follows. The SPIM operation and mathematical model are discussed in section II. In section III, the motor-converter simulation using SimPowerSystems Blockset is detailed. Steady state motor waveforms and current-torque-speed characteristics prediction is discussed in section IV. In section V, the starting inrush current of an SPIM-driven compressor is predicted by simulation and compared to that obtained by experiment. Concluding remarks and future avenues of research are discussed in section VI.

2. Spim Mathematical Model

Most single-phase motors are constructed with two windings which are physically displaced 90 electrical degrees around the motor stator. The windings are often asymmetrical, in which case the "main" winding will have a higher current rating. Furthermore, the "auxiliary" winding is connected to the ac supply through a series capacitor, as shown in Fig.1 to make its current lead the main winding. The series capacitor is ideally chosen so that the main and auxiliary winding currents are time displaced by 90°, achieving exact two-phase operation except for the unbalanced current magnitudes. However, this optimum condition only occurs for a particular motor speed, since the effective impedance of both windings vary significantly with motor slip. Conventional single-phase motors sometimes improve this situation by using two parallel capacitors, in a capacitor-start / capacitor-run configuration, so that exact quadrature time displacement of the currents can occur at least at standstill and at the motors normal operating speed

The following classical assumptions are made in the derivation of the electrical model of the motor [3-8].

- The air-gap is uniform
- Mutual inductance between the two windings is neglected.
- The main and auxiliary stator windings are sinusoidally distributed and arranged in space quadrature.
- The main stator winding (qs winding) is assumed to have N_q equivalent turns.
- The auxiliary stator winding (ds winding) is assumed to have N_d equivalent turns.
- The core loss and saturation are neglected.

It is necessary to transform the variables of the SPIM into a stationary reference frame in order to obtain voltage equations with constant parameters. The rotor bars on d and q axes are short circuited as shown in Fig.2

It is customary to refer the rotor variables to the stator windings by turn ratio. The mathematical model of the SPIM can be expressed with the following equations:

$$V_{qs}^{s} = \left(R_{qs} + \frac{p}{\omega_b} X_{qs} \right) i_{qs}^{s} + \frac{p}{\omega_b} X_{mq} i'^{s}_{qr} \tag{1}$$

$$V_{ds}^{s} = \left(R_{ds} + \frac{p}{\omega_b} X_{ds} \right) i_{ds}^{s} + \frac{p}{\omega_b} X_{md} i'^{s}_{dr} \tag{2}$$

$$0 = \frac{p}{\omega_b} X_{mq} i_{qs}^{s} - \left(\frac{N_q}{N_d} \frac{\omega_r}{\omega_b} X_{md} \right) i_{ds}^{s} + \left(R'_{qr} + \frac{p}{\omega_b} X'_{qr} \right) i'^{s}_{qr} - \left(\frac{N_q}{N_d} \frac{\omega_r}{\omega_b} X'_{dr} \right) i'^{s}_{dr} \tag{3}$$

$$0 = \frac{p}{\omega_b} X_{md} i_{ds}^{s} + \left(\frac{N_d}{N_q} \frac{\omega_r}{\omega_b} X_{mq} \right) i_{qs}^{s} + \left(R'_{dr} + \frac{p}{\omega_b} X'_{dr} \right) i'^{s}_{dr} + \left(\frac{N_d}{N_q} \frac{\omega_r}{\omega_b} X'_{qr} \right) i'^{s}_{qr} \tag{4}$$

$$V_{qs}^{s} = V_s \tag{5}$$

$$V_{ds}^{s} = V_s - \frac{1}{C} \int i_{ds}^{s} dt \tag{6}$$

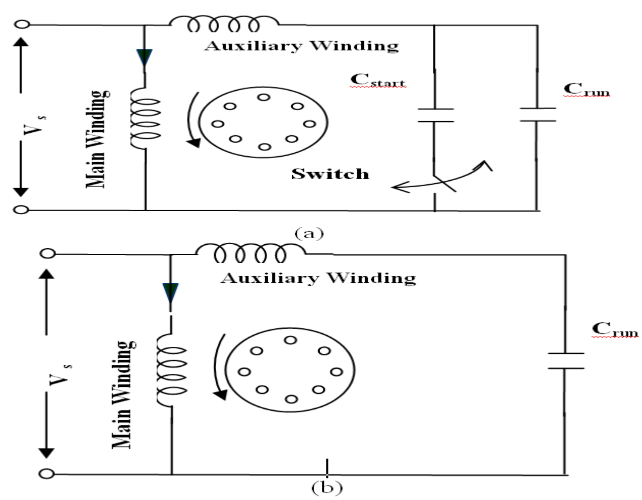

Fig.1. Single phase induction motor (a) Two-Value Capacitor motor, (b) Permanent split motor.

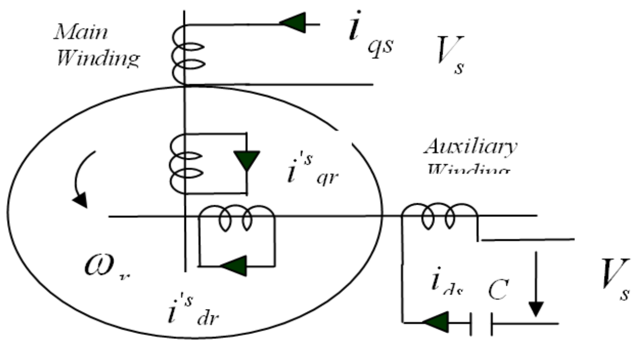

Fig.2. Representation of a capacitor run SPIM in a transformed *dq* stationary reference frame.

Where :

V_s : Supply voltage

V^s_{qs} and V^s_{ds} q^s and d^s axis stator voltage,

i^s_{qs} and i^s_{ds} : q^s and d^s axis stator currents,

i'^s_{qr} and i'^s_{dr} : q^s and d^s axis rotor currents,

R_{qs} and R_{ds} : q^s and d^s axis resistances,

R'_{qr} and R'_{dr} : q^s and d^s axis resistances,

X_{qs} and X_{ds} : q^s and d^s axis stator self reactances,

X_{mq} and X_{md} : q^s and d^s axis magnetizing reactances,

X'_{qr} and X'_{dr} : q^s and d^s axis rotor self reactances,

N_q and N_d : q^s and d^s axis effective turns,

p: differential operator *d/dt*

ω_b : Synchronous angular speed

ω_r : Rotor Electrical Speed

ω_m : Rotor Mechanical Speed

C: capacitor connected in series with the auxiliary winding.

The q^s and d^s axis self reactance can be expressed as:

$$X_{qs} = X_{lqr} + X_{mq} \quad (7)$$

$$X_{ds} = X_{ldr} + X_{md} \quad (8)$$

$$X'_{qr} = X'_{lqr} + X_{mq} \quad (9)$$

$$X'_{dr} = X'_{ldr} + X_{md} \quad (10)$$

Where X_{lqs} and X_{lds} are the q^s and d^s axis stator leakage reactance, X'_{lqr} and X_{ldr} are the q^s and d^s axis rotor leakage reactance.

The instantaneous electromagnetic torque can be expressed as :

$$T_e = \left(\frac{P}{2}\right)\left(\frac{N_d}{N_q}\right)\left(\frac{X_{mq}}{\omega_b}\right)\left(i^s_{qs}\, i'^s_{dr} - i^s_{ds}\, i'^s_{qr}\right) \quad (11)$$

where P is the number of pair of poles for the motor.

The electromechanical equation of the machine is:

$$J_m p\omega_m = (T_e - T_l) \quad (12)$$

where J_m is the inertia constant of motor and load, and T_l is the compressor load torque.

3. Converter-Motor Simulation

If the motor is fed by sinusoidal voltage then equations (1-12) can be easily solved using different well known integration techniques.

As shown in Fig3, all motor differential equations should be transformed into an equivalent electrical circuit.

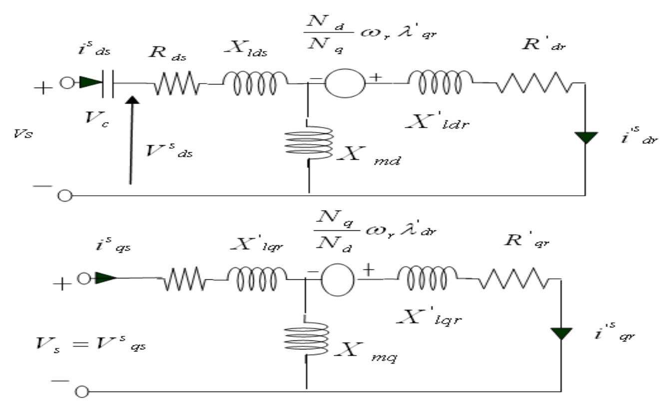

Fig.3. Equivalent electric circuit

A Triac circuit is used to feed both main and auxiliary motor windings. The motor converter coupling is shown in Fig. 4.

When developing improved electrical models, it is important that the user knows what is inside the models Fig.5. By having access to Simulink model, the user can improve the SPIM model or modify its control strategy.

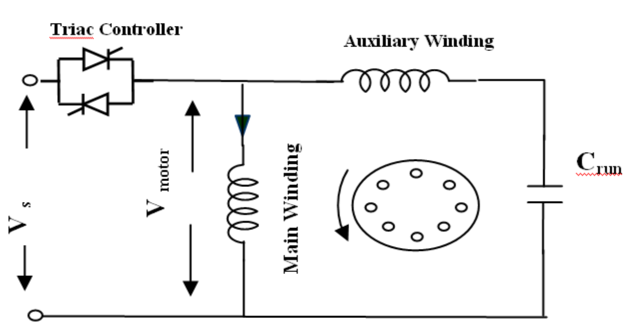

Fig.4. Schematic diagram of the Triac controlled SPIM

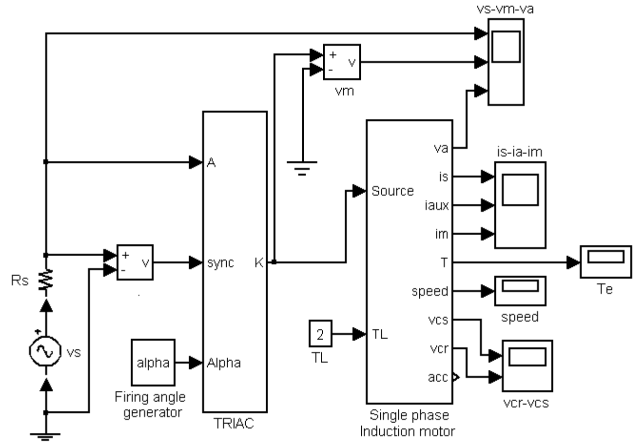

(a)

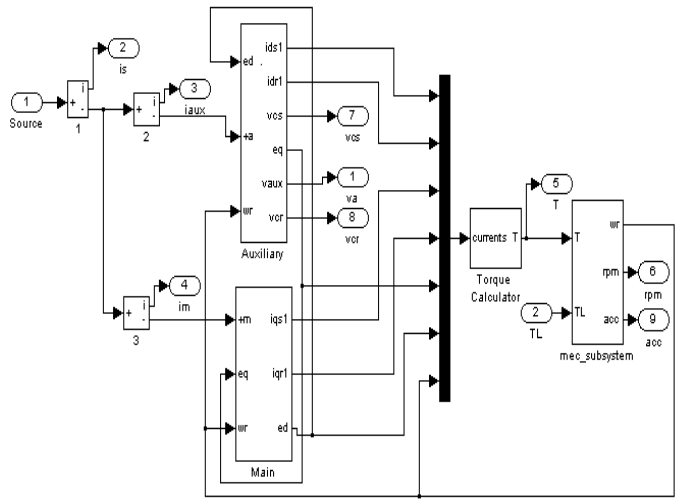

(b)

Fig.5. Simulink Model of a single-phase induction motor.(a) Complete system model,(b) SPIM subsystem model

The simulator allows to data entry of the motor electromagnetic parameters, mechanical load, and converter control parameters through the Simulink Block parameter interface (Fig.6).

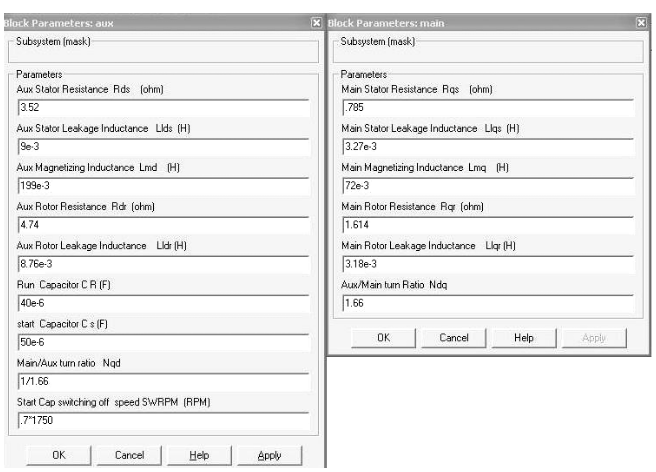
Block Parameters: aux
Subsystem (mask)
Parameters
Aux Stator Resistance Rds (ohm)
3.52
Aux Stator Leakage Inductance Llds (H)
9e-3
Aux Magnetizing Inductance Lmd (H)
199e-3
Aux Rotor Resistance Rdr (ohm)
4.74
Aux Rotor Leakage Inductance Lldr (H)
8.76e-3
Run Capacitor C R (F)
40e-6
start Capacitor C s (F)
50e-6
Main/Aux turn ratio Nqd
1/1.66
Start Cap switching off speed SWRPM (RPM)
.7*1750
OK Cancel Help Apply

Block Parameters: main
Subsystem (mask)
Parameters
Main Stator Resistance Rqs (ohm)
.785
Main Stator Leakage Inductance Llqs (H)
3.27e-3
Main Magnetizing Inductance Lmq (H)
72e-3
Main Rotor Resistance Rqr (ohm)
1.614
Main Rotor Leakage Inductance Llqr (H)
3.18e-3
Aux/Main turn Ratio Ndq
1.66
OK Cancel Help Apply

Fig.6. Main and Auxiliary winding Block parameters

4. Steady State Characteristics

In previous works motor steady state characteristics were obtained using average torque and current expressions derived from the steady-state equivalent model [8]. In this work we propose to use the dynamic simulator for both steady state and transient behavior prediction of the motor-converter system.

By fixing state variables such as rotor speed, prediction of both torque-speed and current-speed characteristics can be performed. Simulation of transient state operation can be conducted by allowing the motor speed to vary according to voltage control inputs.

4.1 Voltage and current waveforms

In order to test the simulator performance in calculating motor waveforms at steady state, simulations were performed for different firing angle. Fig.7 shows the simulated main winding waveforms of voltage and current for a firing angle α=80^o. It is clear to see the main current distortion due high firing angle value.

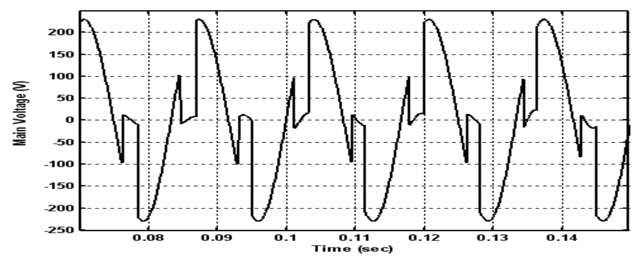

(a)

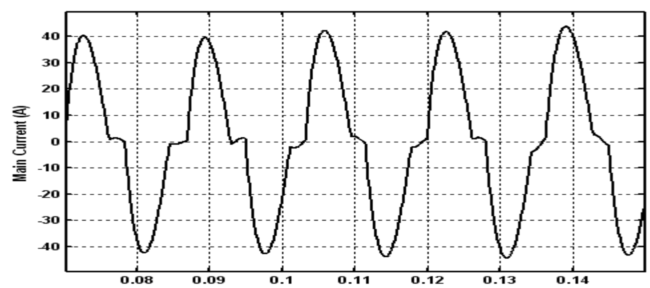

(b)

Fig.7. Main winding waveforms for α=80^o (a) Voltage V^s_{qs}, (b) Current i^s_{qs}.

Fig.8(a). shows the auxiliary winding voltage V^s_{ds}, the auxiliary winding current i^s_{ds} is shown in Fig.8(b) and the capacitor voltage V_c is shown in Fig.8(c). It can be seen that V_c lags i^s_{ds} by 90^o.

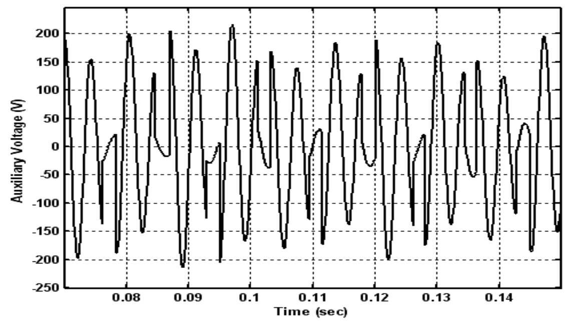

(a)

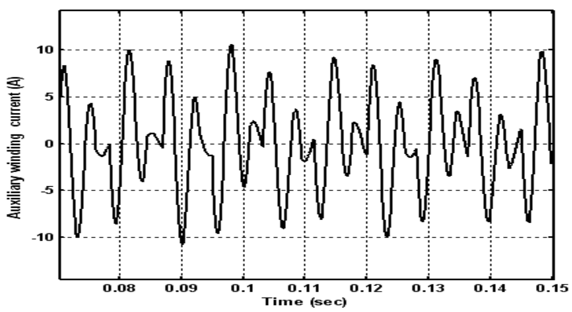

(b)

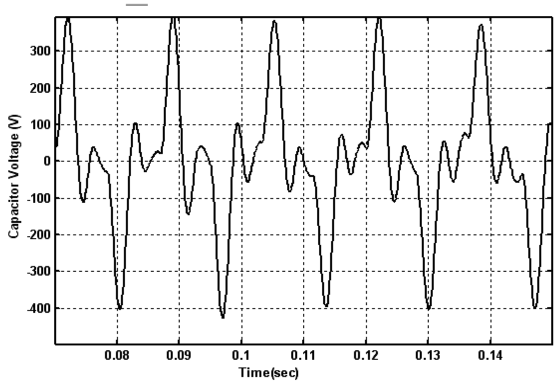

(c)

Fig.8. Auxiliary winding waveforms for $\alpha=80^o$ (a) Voltage V^s_{ds}, (b) Current i^s_{ds}, (c) Capacitor voltage V_c.

4.2 Current-Speed characteristics

Using the simulator we can predict the steady state performances of the motor for different source voltage RMS levels and rotor speeds.

The current-speed characteristic is greatly useful for protection and control design. It shows the RMS motor current demand at different rotor speeds. Fig.9 shows clearly that for a constant RMS voltage, current demand remains high at low speeds and is significantly reduced at speeds near the synchronous speed. Different current curves were obtained by varying the motor RMS value. One can observe that for a large speed range, the current level is greatly affected by RMS voltage. However at speeds near the synchronous speed voltage variation has small effect on motor current.

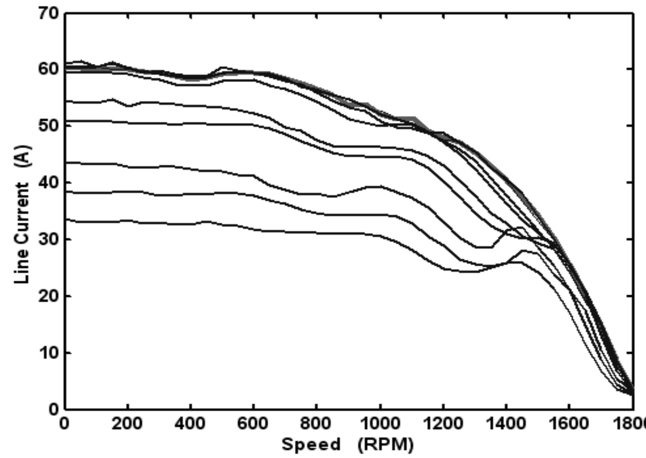

Fig.9. Line current-speed characteristics for different Vs

4.3 Torque-Speed Characteristics

Torque speed characteristics can be predicted for different values of motor RMS voltages. Simulations have been conducted on tow different motor types (the permanent split motor and the tow-value capacitor motor) shown in figure 1. The same run capacitor value was used for both motors. Fig.10 shows torque-speed characteristics obtained for three different RMS voltages (130,160 and 210 V). One can observe that at speeds below 1250 RPM the average torque produced by a tow value capacitor motor is much higher than that produced with a permanent split motor. However beyond that speed the motor's torque capabilities are the same. Such analysis allows determining the required capacitor for speeding up the motor under a certain torque load level.

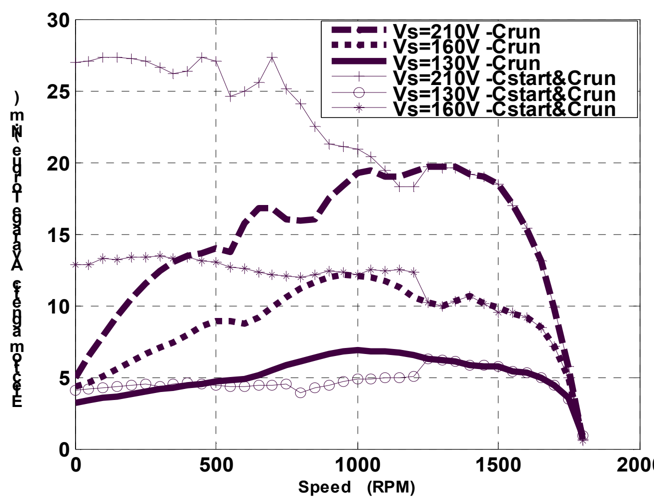

Fig.10. Torque-speed Characteristics for different Vs and starting Capacitors

Based on current and torque-speed characteristics, design of different starting strategies can be performed.

5. Experimental Results

Fig.11 shows the experimental setup used to analyze SPIM performance when started using a Triac circuit. The control circuitry included the synchronization signal generator, interfacing circuit, thyristors firing circuit. The synchronization signal generator is used to generate pulses according to the zero-crossing of the AC signal from the main power supply voltage. The acquisition synchronization circuit waits for the computer signal to start energizing the motor and acquiring the data simultaneously. A signal conditioning circuit is used to scale down the measured signals to voltage levels allowed by the National Instruments data acquisition card. A Desktop Pentium III personal computer was used to run LABVIEW program designed for capturing data from the acquisition card and generating the acquisition-energizing synchronizing signal.

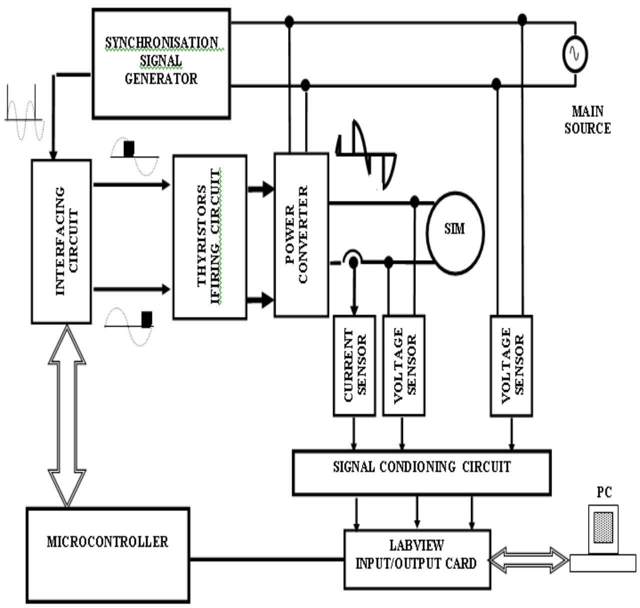

Fig.11. Experimental Setup

Four different channels on the card were used to capture load current, line voltage, load voltage and the firing angle control voltage. The sampling of data was performed at 10 KHz capturing the data for a period of 1.5 seconds for each run. Special care was taken to make sure that the AC run for a certain amount of time before it was switched off and to start the experiment after a delay of approximately five minutes in order to protect the compressor. After the data acquisition was done, Matlab was used for display and result analysis. The PIC16F877 microcontroller was used to initiate the starting of the air-conditioners.

Fig.12. shows both simulation and experimental results obtained for transient current during a direct line AC starting operation. It shows a good agreement between simulated current and current obtained by experiment. As shown in Fig.12(b), saturation effect is observed on current waveform. More accurate current prediction can be achieved if magnetic saturation is considered in motor model.

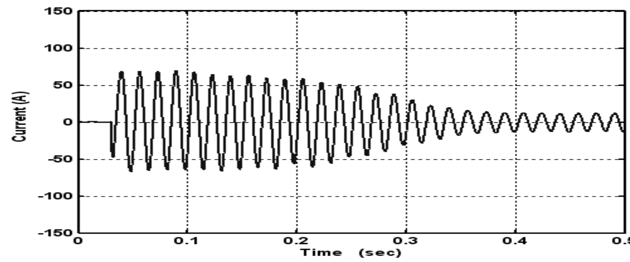

(a)

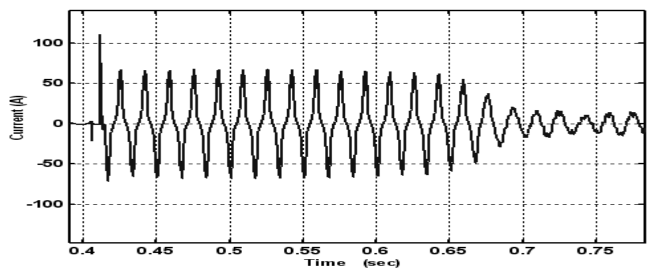

(b)

Fig.12. Line Current (a) Simulated. (b) Measured.

The simulator helps predict the AC starting inrush current when a Triac voltage controller is used for soft starting. Fig.13 shows firing angle variation from 90^o to nearly 20^o during 1 sec.

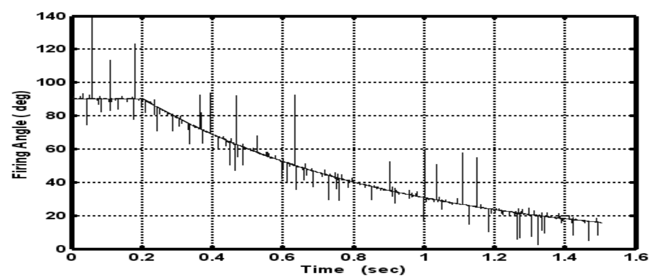

Fig.13. Firing angle variation for soft starting

Fig.14. shows that both simulation and experimental results obtained for transient current during soft starting are in good agreement.

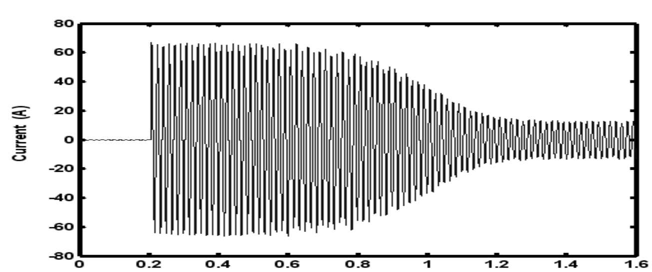

(a)

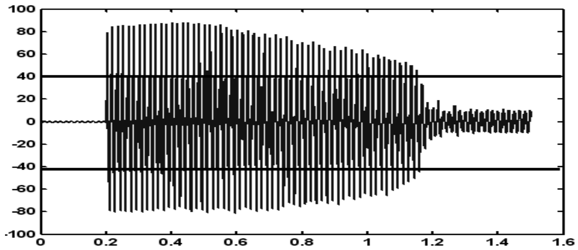

(b)

Fig.14. Inrush current during starting. (a) Simulated, (b) measured.

6. Conclusion

In this paper we presented a SPIM simulator which can simulate both steady state and transient operation. The powerful SimPowerSystems Blockset was used as a simulation platform. Such platform allows the user to include any power converter configuration. The proposed simulator included a Triac based ac power converter used mainly to test the motor-power converter simulator performance.

Both currents and voltage waveforms were simulated. Also, the success in predicting both current-speed and torque-speed characteristics are very helpful for motor control and protection. Direct and soft starting tests were performed on a SPIM driven window type air conditioning unit. Simulations results were compared to those measured through laboratory tests showing a good agreement. This verifies that the proposed simulator is a valid tool for single phase induction motor analysis.

Acknowledgments

This work is supported by the Applied Research Income Grants (ARI Grants) under grant number ARI-043. The authors would also like to acknowledge the support of King Fahd University of Petroleum and Minerals.

References

[1] Rajanathan C.B. and Watson B.J., “Simulation of a single phase induction motor operating in the motoring, generating and braking modes,'' *IEEE Trans.Magn*, vol 32, No. 3, pp. 1541-1544, May, 1996.

[2] Sadowski N., Carlson R., Arruda S.R., Dasilva C.A., and Lajoie-Mazenc M., “Simulation of single-phase induction motor by a general method coupling field and circuit equation,'' *IEEE Trans.Magn.*, vol 31, No. 3, pp. 1908-1911, May, 1995.

[3] Domijan A. and Yin Y., “Single phase induction machine simulation using the electromagnetic transient program: theory and test cases,'' *IEEE Trans. Energy Conversion*., vol 9, No. 3, pp. 535-542, Sept., 1994.

[4] Faiz J. and Keyhani A., “PSPICE simulation of single-phase induction motors,'' *IEEE Trans. Energy Conversion*, vol 14, No. 1, pp. 86-92, March, 1999.

[5] Stankovic A.M., Lesieutre B.C., and Aydin T., “Modeling and analysis of single-phase induction machine with dynamic phasor,'' *IEEE Trans. Power Systems*, vol 14, No. 1, pp. 9-14, Feb., 1999.

[6] Julian A.L., Wallace R.S., and Sood P.K., “Multi-speed control of single-phase induction motor for blower applications,'' *IEEE Trans. Power Elect*., vol 10, No. 1, pp.72-77, Jan., 1995.

[7] Krause P.C., “Simulation of symmetrical induction machinery,'' *IEEE Trans. Power Appar. and Sytems*, vol. Pas-84, No.11, pp. 1038-1053, Nov., 1965.

[8] Liu T.H., “A maximum torque control with a controlled capacitor for a single-phase induction motor,'' *IEEE Trans. Ind. Elect*., vol 42, No. 1, pp. 17-24, Feb., 1995.